DEVELOPMENT OF A NEW STEADY STATE ZERO-DIMENSIONAL SIMULATION MODEL FOR WOODY BIOMASS GASIFICATION IN A FULL SCALE PLANT

Marco Formica[a], Stefano Frigo[b], Roberto Gabbrielli[c*]

[a] Dipartimento di Ingegneria dell'Energia, dei Sistemi, del Territorio e delle Costruzioni - Università di Pisa, Largo L. Lazzarino, 56126 Pisa (Italy), email: marco.formica11@gmail.com

[b] Dipartimento di Ingegneria dell'Energia, dei Sistemi, del Territorio e delle Costruzioni - Università di Pisa, Largo L. Lazzarino, 56126 Pisa (Italy), email: s.frigo@ing.unipi.it

[c] Dipartimento di Ingegneria Civile e Industriale - Università di Pisa, via Bonanno Pisano, 25/b, 56126 Pisa (Italy), phone: +39-050-2217138 email: r.gabbrielli@ing.unipi.it

* corresponding author

ABSTRACT

A new steady state zero-dimensional simulation model for a full-scale woody biomass gasification plant with fixed-bed downdraft gasifier has been developed using Aspen Plus®. The model includes the technical characteristics of all the components (gasifier, cyclone, exchangers, piping, etc.) of the plant and works in accordance with its actual main control logics. Simulation results accord with those obtained during an extensive experimental activity. After the model validation, the influence of operating parameters such as the equivalent ratio, the biomass moisture content and the gasifying air temperature on syngas composition have been analyzed in order to assess the operative behavior and the energy performance of the experimental plant. By recovering the sensible heat of the syngas at the outlet of the gasifier, it is possible to obtain higher values of the gasifying air temperature and an improvement of the overall gasification performances.

Keywords

Downdraft gasifier, Biomass gasification, Steady state simulation, Aspen Plus®, Experimental activity

Nomenclature

CGE [-]: cold gas efficiency

Cp_a [J/kg K]: specific heat of the wind air outside of the gasifier

Cp_i [J/kg K]: specific heat of the air/syngas within chipped biomass bed

$D_{e\_insulation}$ [m]: external diameter of the ceramic fiber insulation

$D_{e\_refractory}$ [m]: external diameter of the protective refractory layer

D_{e_shell} [m]: external diameter of the reactor shell

D_i [m]: internal diameter of the protective refractory layer

d_p [m]: mean equivalent diameter of the chipped biomass that is supposed as sphere

E_m [-]: the emissivity of the cover surface of the external thermal insulation of the gasifier

ER [-]: equivalent ratio

k_a [W/m K]: conductivity of the wind air outside the gasifier

k_i [W/m K]: conductivity of the air/syngas within chipped biomass bed

$k_{insulation}$ [W/m K]: conductivity of the ceramic fiber insulation

$k_{refractory}$ [W/m K]: conductivity of the refractory layer

k_{shell} [W/m K]: conductivity of the shell

L [m]: length of the reactor

l [m]: height of the chipped biomass bed within the gasifier

LHV [kJ/kg]: lower heating value

LHV_b [kJ/kg]: lower heating value of biomass

LHV_s [kJ/kg]: lower heating value of the syngas

MC [-]: moisture content

$\dot{m}_b$ [kg/s]: biomass mass flow

$\dot{m}_s$ [kg/s]: syngas mass flow

m_{a_a} [kg/s]: actual gasifying air mass flow

m_{a_s} [kg/s]: stoichiometric gasifying air mass flow

Nu_a [-]: Nusselt number for the convective heat exchange between the wind air and the cover surface of the external thermal insulation of the gasifier

Nu_i [-]: Nusselt number for the convective heat exchange between the air/syngas and the internal surface of the refractory layer of the gasifier

Pr_a [-]: Prandtl number of the wind air outside of the gasifier

Pr_i [-]: Prandtl number of the air/syngas within chipped biomass bed

$\dot{Q}$ [W]: thermal power that is dispersed by the gasifier into the environment

R_{c1} [K/W]: conductive thermal resistance of the internal refractory layer

R_{c2} [K/W]: conductive thermal resistance of the gasifier shell

R_{c3} [K/W]: conductive thermal resistance of the external thermal insulation of the gasifier shell

R_e [K/W]: thermal resistance of the convective heat exchange between the wind air and the cover surface of the external thermal insulation of the gasifier shell

Re_a [-]: Reynolds number of the wind air outside of the gasifier

Re_i [-]: Reynolds number of the air/syngas within chipped biomass bed

R_i [K/W]: thermal resistance of the convective heat exchange between the air/syngas and the internal surface of the refractory layer of the gasifier

R_r [K/W]: equivalent thermal resistance of the radiative heat exchange between the cover surface of the external thermal insulation of the gasifier shell and the environment

R_{tot} [K/W]: total thermal resistance from the reactor core to the environment

T_e [K]: environment temperature

T_p [K]: the temperature of the cover surface of the external thermal insulation of the gasifier

T_r [K]: mean temperature of air/syngas within the reactor

u_a [m/s]: velocity of the wind air outside of the gasifier

u_i [m/s]: mean velocity of the air/syngas across the chipped biomass bed within the gasifier

Greek symbols

ΔP [Pa]: pressure drop of the air/syngas across the gasifier

ε [-]:mean porosity of the chipped biomass bed within the gasifier

μ_a [kg/m s]: dynamic viscosity of the wind air outside of the gasifier

μ_i [kg/m s]: dynamic viscosity of the air/syngas across the chipped biomass bed within the gasifier

ρ_a [kg/m^3]: density of the wind air outside of the gasifier

ρ_i [kg/m^3]: density of the air/syngas across the chipped biomass bed within the gasifier

σ [W/m^2 K^4]: the Boltzmann constant

1. Introduction

Recently the growing awareness of the shortage of the traditional energy sources and the concern for environmental protection have encouraged the wider use of renewable energy sources. Among these, biomass is certainly one of the most important because of its inexhaustibility and wide availability. In addition, more than wind and photovoltaic, energy conversion of biomass can create concrete local economic opportunities.

The exploitation of energy ~~from~~ through biomass comes off bio-chemical and thermo-chemical processes [1]. Bio-chemical process involves biomethanization of biomass, characterized by low cost effectiveness and efficiency. Actually, the three main thermo-chemical processes are combustion, pyrolysis and gasification. Combustion, apart from the applications in small fireplaces and stoves, is used mainly to supply heat and power ~~with~~ by means of large scale systems (typically above 500 kW_e), and the net efficiency for electricity generation is usually very low and ranges from 15-20 % for the smallest plants (< 1 MW_e) [2]. Pyrolysis converts biomass to bio-fuels and bio-char in absence of oxygen (O_2), but the application of this technology is limited due to the thermal system complexity and the low quality of the fuels that are produced. Gasification [3] converts biomass through a partial oxidation into a gaseous mixture, called *syngas*, and represents, especially in the low power range (< 500 kW_e), the process with the greatest development prospects mainly for its high electric efficiency (20-25 %) [4-5]. Other advantages of gasification are the plant simplicity and the lower capital cost for small scale applications with respect to other technologies. The main drawback is represented by the syngas cleaning system complexity and efficiency.

The development of numerical simulation models is an important tool in order to provide more accurate qualitative and quantitative information on biomass gasification. The possible approaches for the modelling of the gasification process are: steady state models, transient state models and models based on the computational fluid dynamics. The steady state models, that do not consider the time derivatives, are further classified as kinetic rate models and kinetics free equilibrium models [6-9]. For the evaluation of the syngas composition and temperature as function of the process parameters, the kinetics free equilibrium models are the most preferred models because they are very simple and reliable. They have the inherent advantage of being generic but, at the same time, they have thermodynamic limitations, even though researchers have successfully demonstrated that this approach describes sufficiently well the gasification process in downdraft gasifiers [10-13].

A commercial code, such as Aspen Plus®, can be usefully and effectively adopted for the construction of a reliable kinetic free equilibrium simulation model. This article aims at presenting an innovative simulation approach, where the whole experimental gasification plant, containing all the elements such as cyclone, heat exchangers, turbomachineries etc., works following the main control logics of the real plant. Besides, it gives an experimental contribution to the validation of a zero-dimensional steady state simulation model of a full-scale wood-fueled downdraft gasifier. Furthermore, it tries to demonstrate that it is possible to define and tune a reliable equilibrium Aspen Plus® simulation model using detailed experimental data of a real gasification plant (equipment and streams). This model makes it possible to effectively predict the performance of the plant over a wide range of operative conditions.

To the best of the authors' knowledge, simulative models for a whole gasification plant with fixed-bed downdraft gasifier have never presented in literature considering the actual performance characteristics and operative behavior of the plant equipments.

Hence, the work described in this paper is very innovative and can be an useful tool for the developers and users of biomass gasification combined heat and power plants.

On the other hand, there are several papers that describe a steady-state biomass gasification model using Aspen Plus®, mainly in the field of fluidised bed gasifiers. These are briefly summarized below. Ramzan et al. [14] reported an interesting comparative analysis between the simulation performances of a lab-scale up-draft biomass gasifier and the experimental data obtained in literature. Fu et al. [15] analyze without an experimental validation how the performances of an autothermal biomass gasifier are affected by the gasifying air flow and temperature. Doherty et al. [16-18] using experimental data from literature proposed and validated an Aspen Plus® model based on the Gibbs free energy minimisation for a circulating fluidised bed gasifier and for a steam blown dual fluidised bed gasifier, in order to show the dependence of the gasifier performance on the gasifying air temperature.

Several kinds of fluidized bed gasifiers have been simulated and validated using a kinetic model ~~in~~ [19-23], while other authors [24-28] used an equilibrium approach.

A semi detailed kinetic model coupling Aspen Plus® and dedicated fortran subroutines is proposed in [29] for the simulation of an air-steam gasification of biomass in a bubbling fluidised bed. The results of the modelling are well aligned with experimental results available in literature.

Other authors focalized their studies on simulating and validating original two-stage biomass gasifiers [30-31], while in [32] the entrained flow gasification of wood waste is simulated in Aspen Plus® using a plug flow reactor with a kinetic approach. The model validation is executed with experimental results.

In the present work, simulation results have been analyzed and compared with the experimental ones obtained from a commercial-scale gasification plant based on a downdraft gasifier. The plant, with the potential of roughly 80 kW_e, allows to control and adjust many parameters like air flow and temperature into the gasifier or biomass moisture content (MC) and also to measure chemical composition, temperature and flow of syngas coming out from the gasifier.

Using a full-scale experimental biomass gasification plant many operative results were available. This fact allowed both to make a detailed comparative analysis with simulation results and to set some parameters of the model so to achieve an accurate model validation. Inthis paper, after a brief introduction about the gasification principles, the technical and operative characteristics of the full-scale experimental plant are described. Then, Aspen Plus® model of the gasifier and the whole gasification plant are presented. After that, the experimental and simulated data are compared and, successively, the performance assessment of the gasification plant is discussed.

2. GASIFICATION PRINCIPLES

Gasification is a well-known thermochemical process that converts a solid fuel (usually biomass or coal) into a combustible gaseous product (syngas) through partial oxidation, using a gasifying agent in sub stoichiometric conditions [2-3]. When air is used as gasifying agent the syngas consists mainly of carbon monoxide (CO), hydrogen (H_2), carbon dioxide (CO_2), steam (H_2O), methane (CH_4) and nitrogen (N_2) with proportions that depend on air/biomass ratio and MC. In addition there are trace amounts of higher hydrocarbons (such as acetylene, ethene, ethane), and various contaminants such as small char particles, fly ash and tar [33-34].

It is well known that the entire gasification process can be divided into four successive stages: drying, pyrolysis, combustion and gasification [5,9].

In a downdraft fixed bed gasifier, the required heat for the endothermic biomass drying and pyrolysis is provided via heat conduction through the biomass bed by the exothermic combustion zone at the gasifying air inlet. The main reactions in combustion and gasification processes are summarized in Table 1.

The thermodynamic performances of the gasification process can be evaluated using the following parameters:

- the equivalent ratio (ER), defined as follows:

$$ER = \frac{m_{a\_a}}{m_{a\_s}} \quad (1)$$

- cold gas efficiency (CGE), defined as follows:

$$CGE = \frac{\dot{m}_S * LHV_S}{\dot{m}_b * LHV_b} \quad (2)$$

Therefore CGE represents the ratio between the inlet biomass chemical energy and the corresponding chemical value of the syngas.

Table 1 Main gasification reactions.

Heterogeneous reactions:		
$C_{(s)} + O_{2(v)} \rightarrow CO_{2\,(v)} + 394$ kJ/mol	C complete combustion	(R1)
$C_{(s)} + 0.5\ O_{2(v)} \rightarrow CO_{(v)} + 111$ kJ/mol	*C partial combustion*	(R2)
$C_{(s)} + CO_{2(v)} \rightarrow 2\ CO_{(v)} - 172$ kJ/mol	*Boudouard*	(R3)
$C_{(s)} + H_2O_{(v)} \rightarrow CO_{(v)} + H_2 - 131$ kJ/mol	*Water-gas*	(R4)
$C_{(s)} + 2\ H_{2(v)} \rightarrow CH_{4(v)} + 75$ kJ/mol	*Methanation*	(R5)
Homogeneous reactions:		
$CO_{(v)} + 0.5\ O_{2(v)} \rightarrow CO_{2(v)} + 283$ kJ/mol	*CO partial combustion*	(R6)
$H_{2(v)} + 0.5\ O_{2(v)} \rightarrow H_2O_{(v)} + 242$ kJ/mol	*H_2 combustion*	(R7)
$CO_{(v)} + H_2O_{(v)} \rightarrow CO_{2(v)} + H_2 + 41$ kJ/mol	*CO shift*	(R8)
$CH_{4(v)} + H_2O_{(v)} \rightarrow CO_{(v)} + 3\ H_2 - 206$ kJ/mol	*Steam-methane reforming*	(R9)
H_2S and NH_3 formation reactions:		

$H_{2(v)} + S_{(s)} \rightarrow H_2S_{(v)}$	*H_2S formation*	(R10)
$N_{2(v)} + 3\ H_{2(v)} \rightarrow 2\ NH_{3(v)}$	*NH_3 formation*	(R11)

3. THE EXPERIMENTAL GASIFICATION PLANT

3.1 Layout

The experimental gasification plant (Figure 1) is the result of a long research activity that has been performed at the “Dipartimento di Ingegneria Civile e Industriale” (DICI) and “Dipartimento di Ingegneria dell’Energia, dei Sistemi, del Territorio e delle Costruzioni” (DESTEC) of the University of Pisa (Italy).

The virgin chipped biomass is dried using a stand-alone concurrent rotating dryer that is equipped, to accomplish the drying process, with a LPG fired burner. In a future commercial configuration, the hot exhaust gas of the internal combustion engine fuelled by syngas will be used for drying. Periodically, a sample of dried chips is analysed to evaluate its MC and composition.

The dry wood chips are then filled into the gasifier using a screw conveyor and a rotary valve, while the air flow coming into the gasifier is preheated initially through an electric preheater (during the starting of the gasification plant when the syngas temperature is not enough high). Later, when the steady state regime is reached, the air is heated passing through a shell-and-tube heat recuperator, where the high-temperature syngas at the outlet of the gasifier is cooled. In order to avoid the ~~obstruction~~ blockage of the syngas outlet section, and consequently the stoppage of the reactor, the unburnt char is periodically extracted from the gasifier.

~~The syngas light carbonaceous residues~~ The char residues and fly ash are removed from the syngas in a cyclone. The syngas is further cooled in a second air-cooled shell-and-tube heat exchanger. In the experimental facility this cooling air is dispersed into the atmosphere, but in a commercial layout of the gasification plant the sensible heat of the syngas could be effectively recovered for cogeneration application. At the outlet of the cooler, the contents of pollutants in the syngas, such as fly ash and tar, are lowered using a custom-made filter. Then, the syngas passes through the suction fan, which is responsible of the gasifying air-syngas flow.

The syngas is finally oxidized in a custom combustion chamber equipped with a LPG burner. This special combustion chamber has been adopted in place of a conventional torch for safety reasons, since it ensures long residence time of CO at high temperatures and, consequently, its complete oxidation. In the commercial version of the plant an internal combustion engine in combination with a torch will replace the combustion chamber. The torch will be used to oxidize the syngas when the quality of the gas is not suitable for the engine (for example, during the plant starting) or when the engine does not work due to failures.

The operation of the experimental gasification plant is supervised by a programmable logic controller (PLC) that can be managed by the user with a user-friendly touch screen system. The temperature and pressure of each stream are measured and the measurement signals are connected to the PLC system. Moreover, air and syngas flows are continuously measured via two dedicated Honeywell flow transmitters (the syngas one includes the compensation of temperature) based on the orifice plate method.

Using some sampling points located in different places along the syngas stream line, it is possible to extract the syngas in order to evaluate its macro-components with an off-line gaschromatograph and also tar and ash content via a sampling probe. This probe was designed and constructed in accordance with the tar Protocol [35-36].

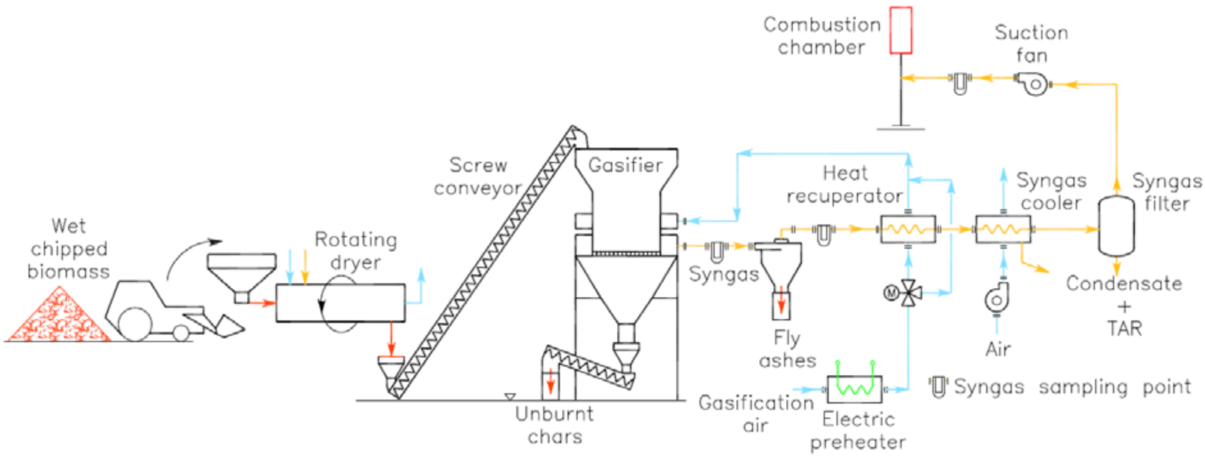

Figure 1 Layout of the biomass gasification power plant.

The most important design data of the experimental plant are summarized below:

- biomass mass flow feeding the gasifier with MC of 10 %: 90 kg/h
- gasifying air temperature at the inlet of the gasifier: 450 °C
- syngas mass flow: 200 kg/h
- syngas temperature at the inlet of the suction fan: 75 °C.

3.2 Main control logics for the operative management of the experimental gasification plant

The experimental gasification plant operates in accordance with some fundamental control logics that were implemented and managed by a governing PLC. These ~~rules~~ logics assure large flexibility from the operative point of view and the possibility to test different configurations. In particular the logics are:

1. automatic adjustment of the opening of the motorized three way valve located upstream of the heat recuperator (air-side) so that the air temperature just upstream the gasifier reaches a specified set-point value;
2. the cooling air mass flow in the syngas cooler is tuned by modifying the rotational speed of the fan via electric motor inverter, in order to obtain a set-point value of the syngas temperature at the outlet of the cooler;
3. gasification flow logic: the speed of the syngas suction fan is modified via electric motor inverter in order to obtain a specified syngas mass flow upstream the combustion chamber. Similarly the logic can be modified using a set-point of the gasifying air mass flow as control objective;
4. the filling of the reactor starts periodically in accordance with a time log and stops when the level of the biomass chips inside the gasifier reaches the highest allowable level activating a blade sensor level;
5. the unburned char is periodically discharged in order to avoid the blockage of the reactor when the pressure drop across the reactor reaches the set-point level and then extracted with a dedicated screw conveyor.

4. ASPEN PLUS® MODEL

Referring to the plant layout (Figure 1) the simulation flowsheet of the plant (Figure 2) has been created.

4.1 Gasifier

A kinetic free equilibrium steady state model has been developed for the gasification process. Initially the model simulates the biomass drying, reducing its MC up to a predetermined value.

Afterwards, biomass is decomposed into volatile components and char and then oxidation and gasification reactions are simulated by minimizing Gibbs free energy.

The block DRIER1 has been used to reduce the MC of moist biomass, simulating biomass drying controlled by a Fortran ~~statement~~ routine. Excess water is separated in the block DRYER2 (Sep type), while dry biomass with the right MC at the inlet of the gasification reactor is then decomposed into its conventional elements (C, H, O, N, S etc.) in the block DECO (Ryield type), that uses calculations based on the component yield specification, controlled by a Fortran statement. Ash and specified percentage of carbon of the dry biomass are separated in the block CHAR-SEP (Sep type) in order to simulate the unburnt char that is extracted from the bottom of the gasifier. The remaining elements are carried with the heat of reaction associated with the decomposition of the biomass into the block GASIFIER (RGibbs type), where the preheated gasifying air enters and the combustion and gasification reactions occur. The gasification products are calculated by minimizing the Gibbs free energy and assuming complete chemical equilibrium. Finally, taking into account the reactor geometry and thermal insulation, pressure drop across the gasifier and heat losses to the ambient are calculated with a user routine (see Appendix A).

Biomass is specified as a non-conventional component, with a chemical composition defined by the ultimate and proximate analysis in accordance with the results of the laboratory analysis, as shown in Table 2.

Table 2 Ultimate and proximate analyses of chestnut wood.

Proximate Analysis		**Ultimate Analysis**	
Moisture	10 %	Carbon	50.96 %

Fixed Carbon	50 %	Hydrogen	5.978 %
Volatile Matter	48 %	Nitrogen	0.49 %
Ash	2 %	Chlorine	0.0098 %
		Sulphur	0.0392 %
		Oxygen	40.523 %
		Ash	2 %

4.2 Other equipment

In order to reproduce the thermodynamic plant operation accurately and, after an experimental validation, to predict the behavior of the system in general operating conditions, the geometrical and operative characteristics of the equipment that are actually installed at the experimental facility have been inserted within the simulation model. In particular:

- pressure drop ratio factor, the pressure recovery factor and the valve flow coefficient of the valves (VA01, 3W-VALVE, VG01, VG02 in Figure 2) have been specified in accordance with the real data from the equipment datasheets. In this way it is possible to predict the pressure drop of the valve as a function of its geometrical dimensions and percent opening;
- geometrical data, such as internal diameter, length and material have been inserted for the piping (PIPE-1, PIPE-2, PIPE-3 in Figure 2). Further, with the addition of the calculator tool of Aspen Plus®, the heat losses to the ambient have been calculated in function of the actual insulation characteristics, the ambient air temperature and wind speed during the experimental tests;
- the geometry of the heat exchangers (HEATER and E02 in Figure 2) has been designed using the specific code of Aspen Plus® for the shell and tube heat exchangers and their simulation model has been ~~linked within that of the gasification plant~~ implemented into the main one.

In this way it is possible to assess the real thermodynamic off-design performance of the heater when the operating conditions change with respect to the design point. The electric heater (E-HEATER in Figure 2) has been simulated using a particular user routine in order to assess its actual thermal performance in function of the thermal load and air mass flow. The heat losses of the heaters to the environment have been calculated in function of their specific geometry and the insulation characteristics;

- geometrical data of the cyclone (CYCLONE in Figure 2) have been ~~inserted~~ considered in order to assess its fly ash separation performance. A specific routine has been added in order to evaluate the heat loss to the environment, adopting the approach described above for the piping and inserting a heater block (D01-Q-P in Figure 2) downstream the cyclone;
- the simulation of the air and syngas fans (AIR-FAN and S-FAN in Figure 2) has been executed inserting their characteristic curves in terms of head and efficiency as a function of flow at different shaft rotational speeds in accordance with the manufacturer datasheets. The actual operating speed of the fans is calculated once the flow and the head have been evaluated in agreement with the control logics described in the previous section and assuring the gas flow with the calculated pressure drop, respectively;
- the final complete oxidation of the syngas within the combustion chamber (CC in Figure 2) has been simulated using a RGibbs type block. The pressure loss through the combustion chamber has been inserted as an input of the model using the experimental data. The overall chemical power that is associated with the syngas flow is calculated via the cooling of the combustion products with a heater block (QSYNGAS in Figure 2);
- the simulation of the syngas filter (COOLER in Figure 2) that is positioned upstream the fan is executed using a separation block (Sep type) with a pressure loss that has been experimentally evaluated in function of the actual syngas flow;

- the air and syngas flowmeters (F01 and F02 in Figure 2), which are based on the orifice plate technology, have been simulated with valves whose pressure losses are in accordance with formulation reported in [37] as function of the volume flow.

The control logics of the experimental plant have been implemented in the simulation model using the Design Specs tool of Aspen Plus®. In this way it is possible to find the value of one or more control variables, such as, for example, the motor speed of the syngas fan, in order to iteratively reach a specified goal, such as the syngas mass flow.

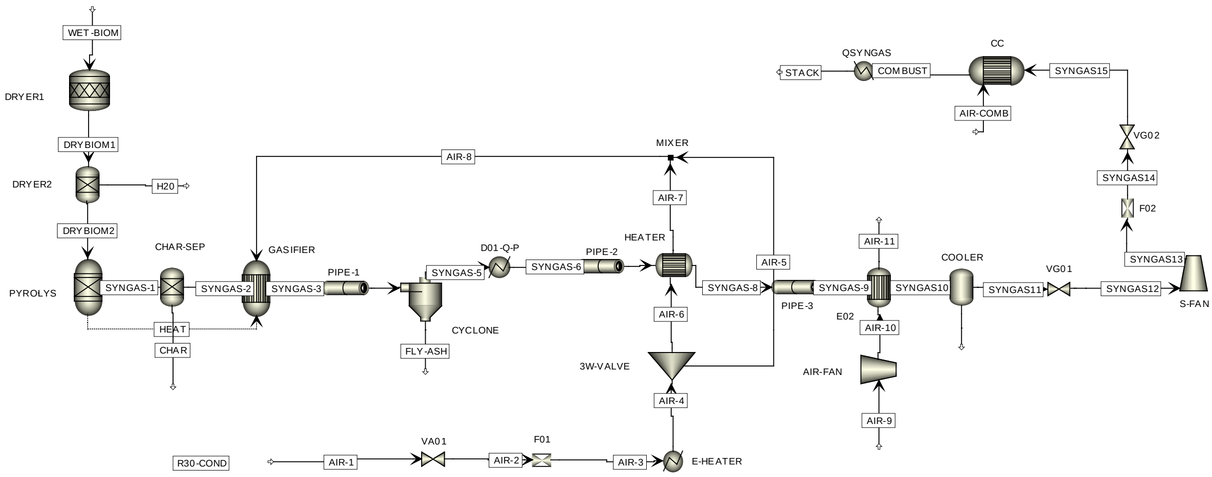

Figure 2 Aspen Plus® simulation model of the experimental gasification plant.

4.3 Physical property method

The equation of state that is used to estimate all physical properties of the conventional components is the Peng-Robinson equation with Boston-Mathias alpha function (PR-BM), which is appropriate for gasification processes where temperature is quite high.

4.4 Simplifying assumptions

Within the model some simplifying assumptions that do not markedly affect the goodness of the simulation results are:

- steady state conditions: as demonstrated by the experimental data, after roughly two hours from the starting of the gasification reactions, the temperature profile within each equipment, such as the gasifier and the heat exchangers, fluctuates slightly. This assures that the operating conditions do not practically change in time.
- kinetic free model: as stated in the Introduction, the estimation of reliable kinetic data for the specific gasification configuration can be an hard task without assuring the goodness of the results. The adoption of the equilibrium approach in combination with a detailed geometrical simulation of the plant equipment can assure in any case to obtain a good representation of the experimental data;
- the sulphur reacts forming H_2S, as demonstrated by the experimental analysis;
- no nitrogen oxides are considered and N_2 forms only NH_3: the study of the formation of the micro-pollutant is not an objective of the paper. They do not affect the overall energy balance of the gasifier and the macro-composition of the syngas;
- the formation of the tars and other heavy products at equilibrium conditions are not simulated. It is important to note that their influence on the overall energy balance of the gasifier is marginal.

5. Results and Discussion

5.1 Experimental activity vs simulation results

Several different operative conditions have been considered during the experimental activity, varying the ER (modifying the suction fan rotational speed and consequently the air mass flows) and the gasifying air temperature at the inlet of the reactor (changing the opening of the bypass valve of the air preheater). As stated above, the thermodynamic data of each stream of the plant, the biomass characteristics and the syngas composition have been measured during the tests. Some experimental data have been used as inputs of the Aspen Plus® simulation model. In particular:

- the ambient gasifying air: temperature, pressure, relative humidity and mass flow, temperature at the inlet of the gasifier;
- biomass: chemical composition, MC, mass flow;
- syngas: temperature at the outlet of the cooler;
- unburnt char that is extracted from the bottom of the gasifier: mass flow, chemical composition;
- fly ashes from the gasifier: size distribution, concentration.

Using these inputs, the simulation model calculates the syngas composition, temperature and mass flow at each point of the plant (and consequently the rotational speed of each fan), the thermal power of each heat exchanger, the aperture of the control valve of the air preheater. The comparison of the experimental data and the results of the simulations, that have been executed using data of about twenty experimental tests (Appendix B), are reported in Figures 3, 4, 5, 6 and 7. The trend and the values of the mass composition of the syngas are well simulated by Aspen Plus® and the percentage error is marginal, also considering the intrinsic error of the experimental measurements, which can be summarized in the following:

(i) the measurements of the temperature that are executed using thermocouples of type K have a standard intrinsic tolerance of ± 6 %;

(ii) the mass flow of the biomass has not been continuously monitored, but it is evaluated measuring in average the biomass that is consumed;

(iii) the MC of biomass, that is not an homogeneous fuel, is not evidently measured in continuous way, but some representative samples have been analysed. Some MC differences between the measurement instant and the moment of gasification are inevitable due to the fact that the material is not homogeneous and some moisture is slightly absorbed from the environment;

(iv) as the experimental experience of the authors, the syngas composition is not perfectly stable and fluctuates due to the fact that the biomass within the gasification bed is evidently heterogeneous and the air and syngas fluid-dynamic through the biomass is affected by inevitable variations;

(v) the volume flow measurement of air and syngas is affected by an error by about ± 1 %;

(vi) there are inevitable errors of the laboratory measurements that can be estimate equal to about ± 0.5 %.

The average value and the standard deviation of the percentage difference between the experimental and simulated results are summarized in Table 3. The parity plot of the molar composition between the simulated values and the experimental ones, reported in Figure 8, allows to assess the prediction accuracy of the simulation model. The average differences between the measured LHV of the syngas and the simulated values and between the experimental CGE and the simulated ones as well are about 7 % and 5 %, respectively.

Moreover, the average difference between the simulated values of the syngas temperature at the outlet of the gasifier and the experimental values is lower than 7 %. On the basis of these negligible differences, the Aspen simulation model can be considered particularly accurate for the estimation of the most important energy performance indicators and operative data of the experimental facility. The most relevant difference between the experimental and simulated results concern the mass and molar concentration of H_2, that is overestimated, and CH_4, that is underestimated. Using the equilibrium hypothesis in the simulation model, the conversion of the methane into hydrogen, which depends on the actual crossing time of the gasification bed, is overestimated. Indeed, the methane that is produced during the pyrolysis is progressively converted along the gasifying bed into H_2 and CO in accordance with the steam reforming reaction. Using the hypothesis of equilibrium, the steam reforming reaction is completed shifted toward the products, as reported also by other authors [38-39]. This condition is hardly confirmed in real situations. However, it is important to note that the differences are lower with higher values of ER, when the hypothesis of equilibrium is more respected. Moreover, considering the overall amount of hydrogen moles and mass the differences reduce largely (Table 3).

However, as a whole, the dependence of the syngas composition on the ER is in good agreement with the values of literature [7, 40-41]. Notwithstanding this difference for the H_2 estimation, the results concerning the plant operation and its energy balance are well simulated by the Aspen Plus® model.

In general, the increasing ER implies a larger extension of the combustion process within the reactor (hence the temperature inside the reactor increases, as shown in Figure 5), with a lower content of the combustible components in favor of the nitrogen content that increases. When the gasifying air increases, the LHV of the syngas consequently decreases (Figure 7) due to the oxidation of the hydrogen and CO and the dilution due to the nitrogen. Consequently, CGE decreases with ER (see Figure 7), too.

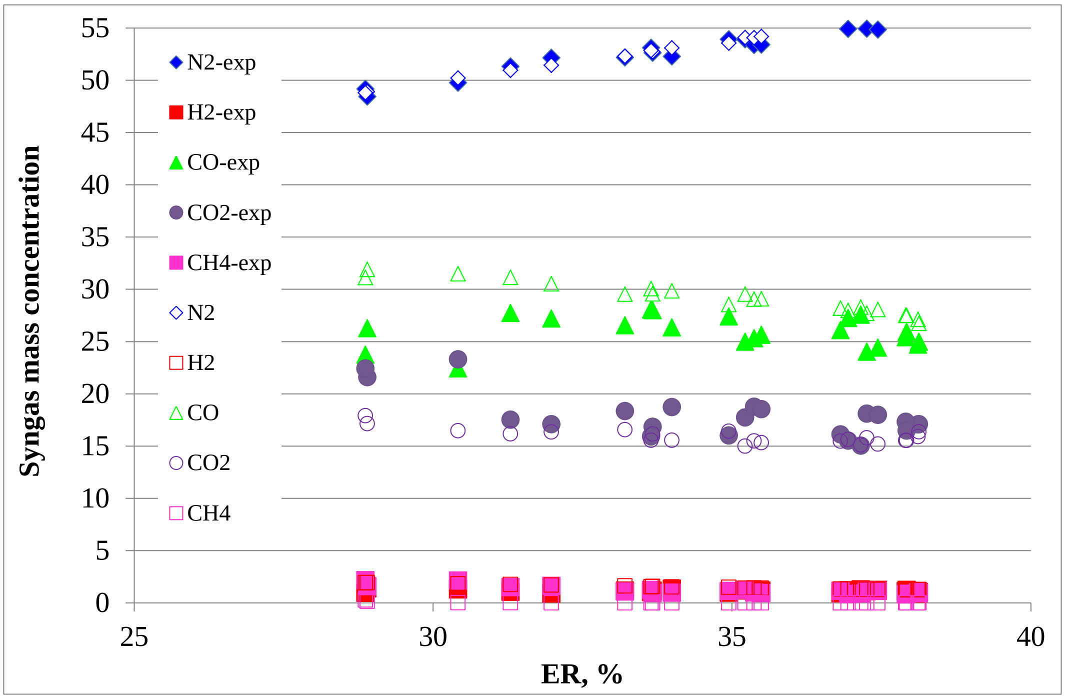

Figure 3 Comparison of the experimental syngas mass composition (labelled with "exp") with the results of the Aspen Plus® simulation model (dry basis).

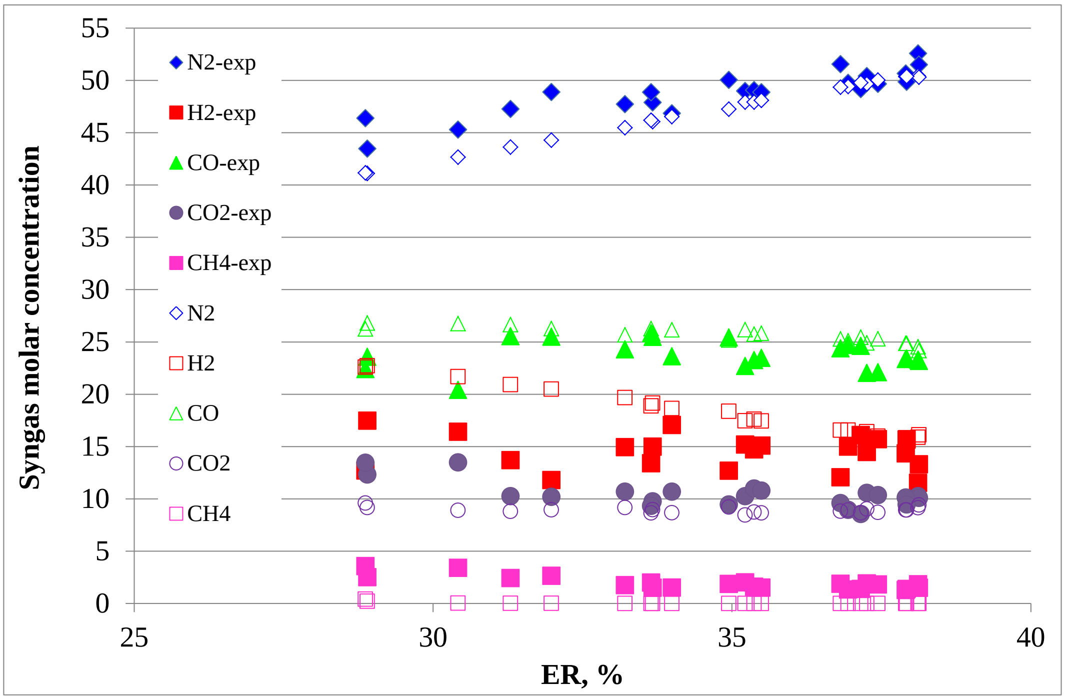

Figure 4 Comparison of the experimental syngas molar composition (labelled with "exp") with the results of the Aspen Plus® simulation model (dry basis).

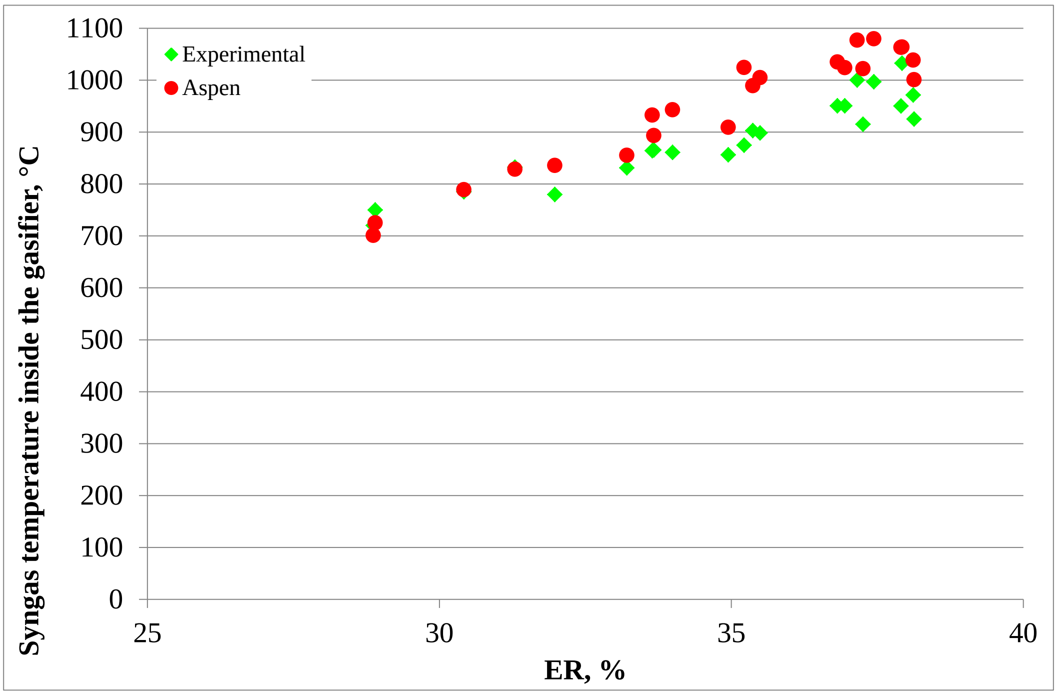

Figure 5 Comparison of the experimental syngas temperature inside the gasifier with the results of the Aspen Plus® simulation model.

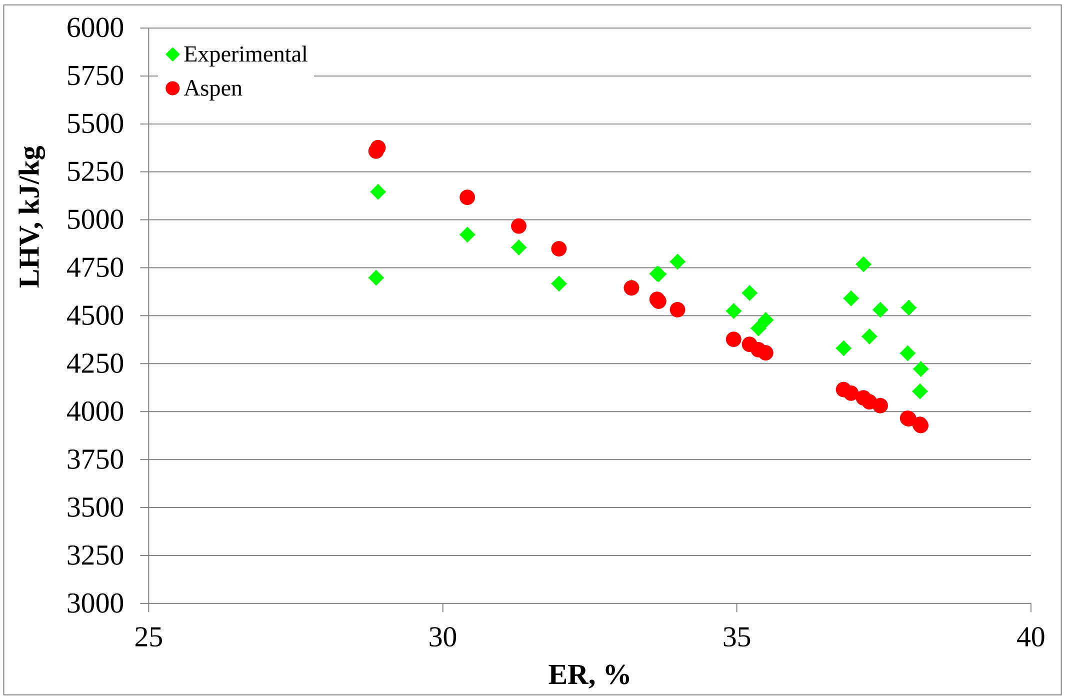

Figure 6 Comparison of the experimental syngas lower heating value with the results of the Aspen Plus® simulation model.

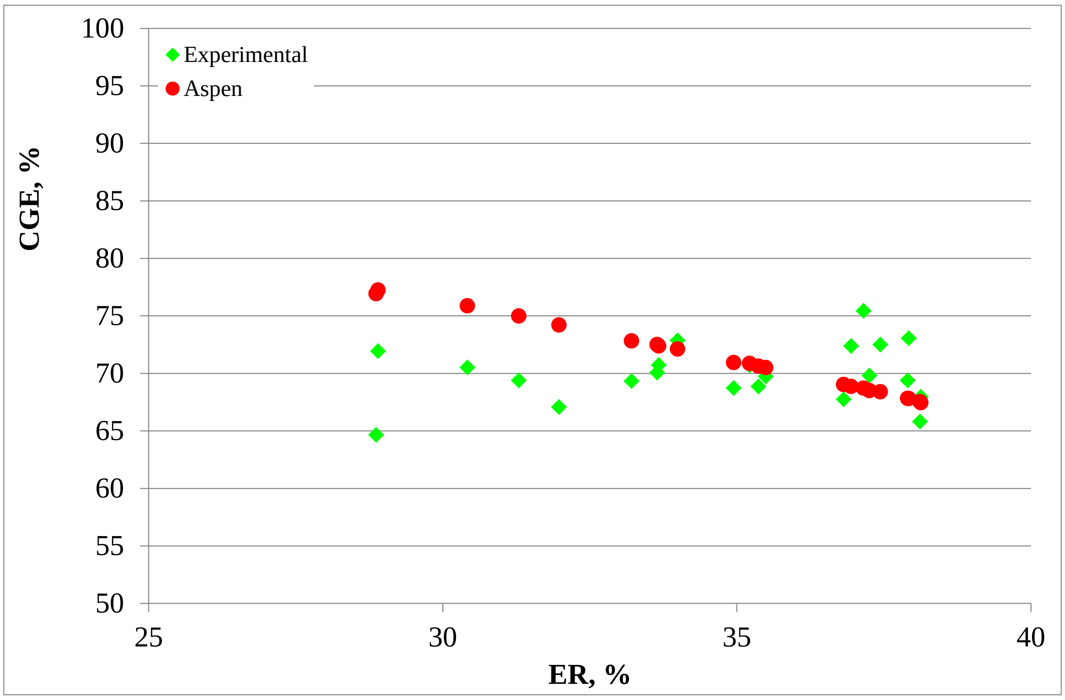

Figure 7 Comparison of the experimental cold gas efficiency with the results of the Aspen Plus® simulation model.

Table 3 Average value and standard deviation of the percentage difference between the experimental and simulated results.

	Syngas mass concentration				
	N_2	H_2	CO	CO_2	CH_4
Average	0.7	35.2	12.2	10.2	95.9
Standard deviation	0.4	27.4	9.1	7.7	14.9
	Syngas molar concentration				
	N_2	H_2	CO	CO_2	CH_4
Average	4.0	29.0	8.4	13.1	95.5
Standard deviation	3.1	22.2	7.0	8.8	17.1
	CGE	LHV	Syngas temperature	H_2 mass	H_2 mole
Average	5.5	6.6	6.3	13.2	4.6
Standard deviation	5.2	4.5	5.1	12.6	3.4

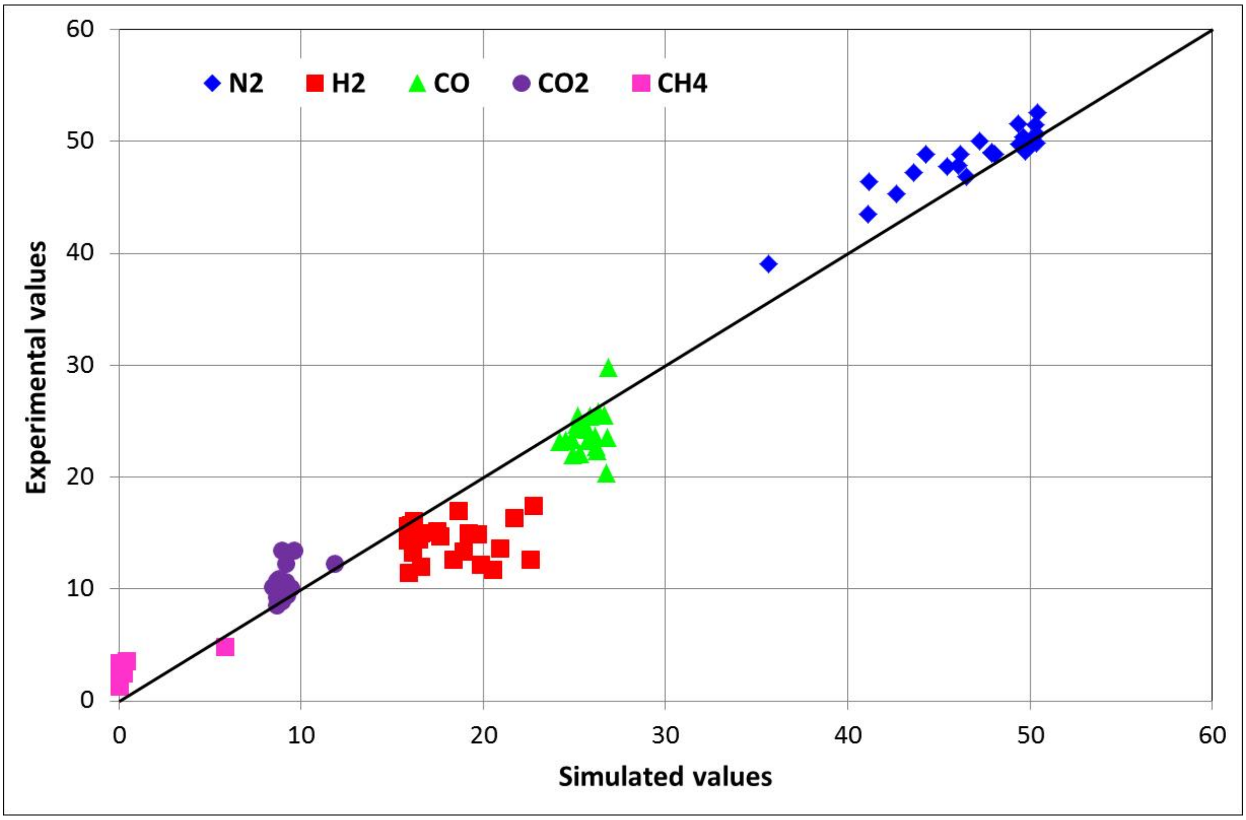

Figure 8 Parity plot for the molar composition of the syngas (dry basis).

5.2 Performance assessment of the experimental gasification plant with Aspen Plus®

Once the reliability of the simulation model has been demonstrated using the comparison with the experimental data, it is possible to use it to predict and assess the thermodynamic and energy performance of the experimental gasification plant in various operative conditions without the necessity to execute further experimental tests. The most important controllable parameters for the gasification plant user are:

- the MC of the biomass, that can largely vary from a supply to another. Indeed, the wood chipped biomass can contain variable amount of the water during the year and the drier cannot assure a constant MC of the dried biomass;
- the ER that largely affects the gasification efficiency and the syngas composition. It is the

most simple controllable plant parameter that the user can easily modify, operating the suction fan;

- the gasifying air temperature, that can be simply modified with the control valve and affects the overall thermal performance of the gasification plant.

Hence, the simulations have been executed at different values of biomass MC and gasifying air temperature vs. ER. In particular, two extreme values have been adopted for the biomass MC (6 % and 14 %) and for the gasifying air temperature (20 °C and 300 °C). When the MC of biomass has been increased, we assumed to maintain constant its dry matter mass flow equal to 72 kg/h. The lowest value of the biomass MC can be considered the lower bound that can be practically obtained using commercial industrial driers. The highest value is generally considered the maximum allowable value in order to avoid an excessive production of tar in the syngas. The maximum value of the gasifying air temperature can be easily obtained using the air preheating with suitable gas-gas heat exchangers. The lowest value, that corresponds to the atmospheric temperature, represents the absence of the air preheating and the heat exchanger is completely bypassed by the air. So, ambient air is directly used as gasifying agent. In this case the sensible heat of the syngas can be recovered during the successive cooling with the atmospheric air.

The reduction of the biomass MC (Figures 9 and 10) ensures a higher production of CO, with an increase in LHV_s (Figure 11) and CGE (Figure 12). Indeed, the absorption of latent heat (required for the water vaporization) reduces the useful heat for the gasification reaction and the presence of steam tends to dilute the syngas. The value of ER with the highest H_2 and CO content in the syngas is slightly lower with high gasifying air temperature (Figures 9 and 10).

Figures 11 and 12 show that the reduction of ER increases syngas LHV and CGE, so the adoption of low ER could be reasonable. Actually the model-does not take into consideration tar production which drastically increases at the lowest ER. Usually, an ER around 25-30 % is adopted during operative conditions.

The effect of the gasifying air temperature on the gasifier performance is more relevant in comparison with the MC (Figures 9, 10, 11, 12). On average, the change of the gasifying air temperature from 20 °C to 300 °C implies the increase of the gasification efficiency by about two percentage points. High values of the temperature assure an effective heating of the biomass bed within the reactor and a more efficient development of the gasification reactions with a higher syngas outlet temperature, as shown in Figure 13, and consequently higher biomass conversion into syngas. Moreover, the syngas outlet temperature (Figure 13) can be higher when the biomass has a low MC and, consequently, a higher LHV. With a low value of MC it is possible to obtain higher gasification efficiencies as it happens increasing the air inlet temperature. In particular, the change of MC from 6 % to 14 % implies the increase of the gasification efficiency by about one percentage point.

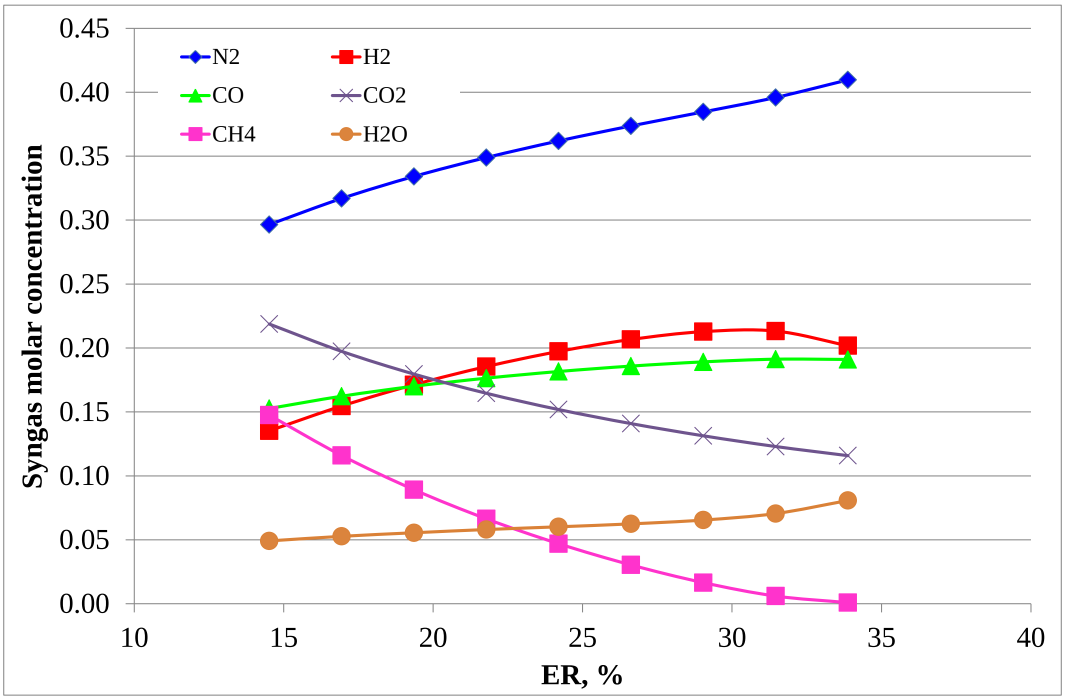

(a)

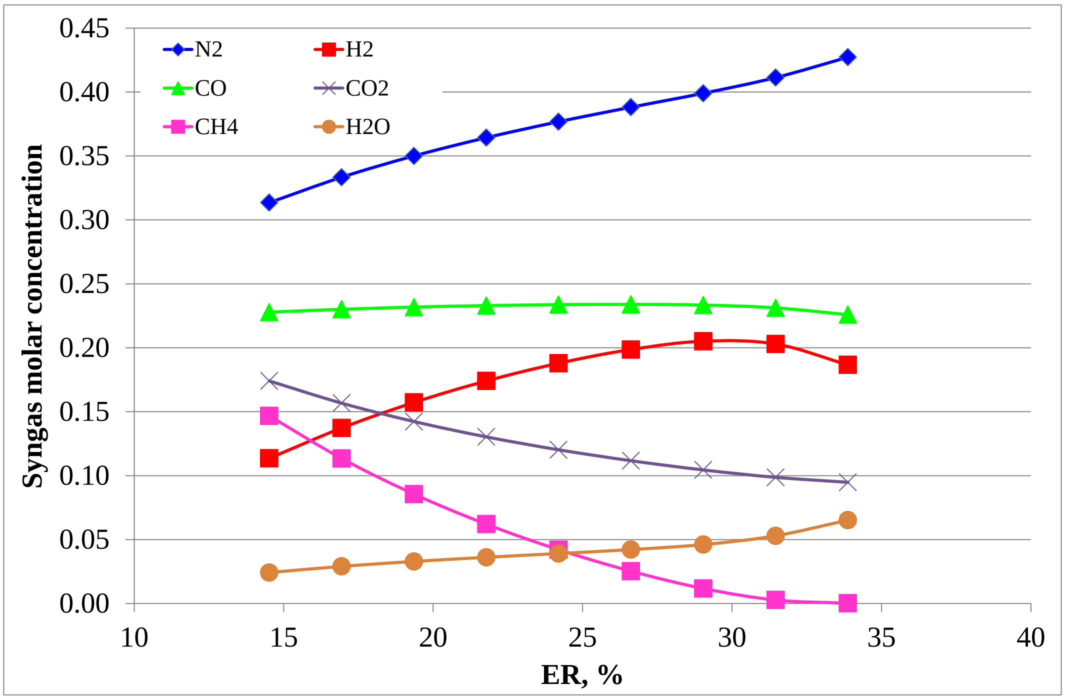

(b)

Figure 9 Syngas composition with the Aspen Plus® model, when the biomass moisture content is equal to 14 % (a) and 6 % (b) and the gasifying air temperature is equal to 20 °C.

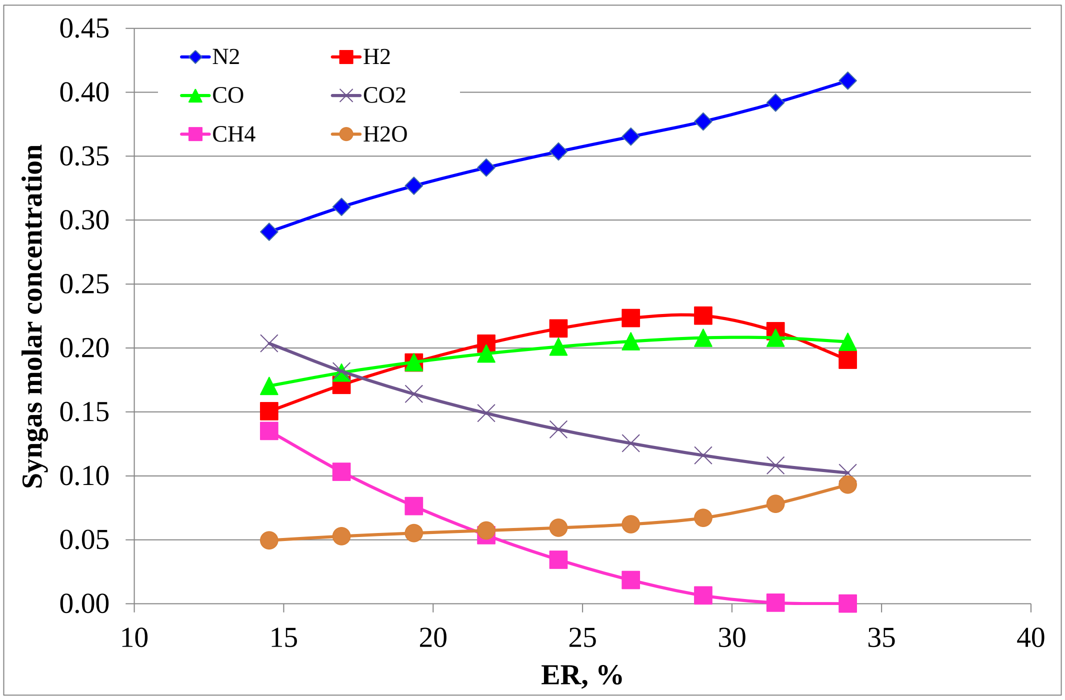

(a)

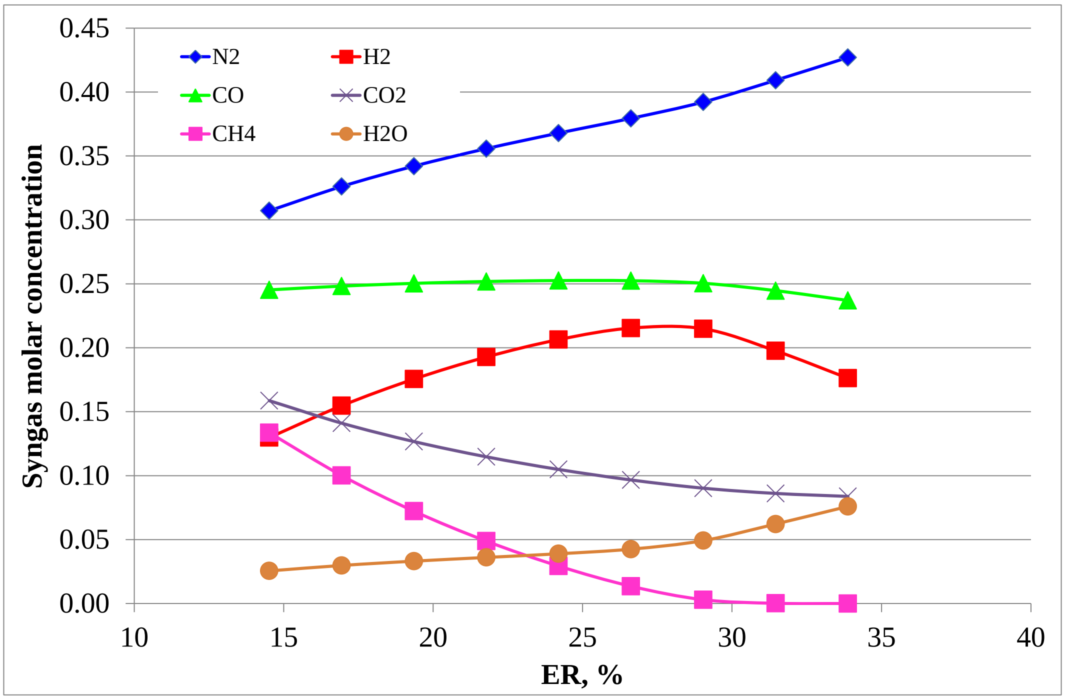

(b)

Figure 10 Syngas composition with the Aspen Plus® model, when the biomass moisture content is equal to 14 % (a) and 6 % (b) and the gasifying air temperature is equal to 300 °C.

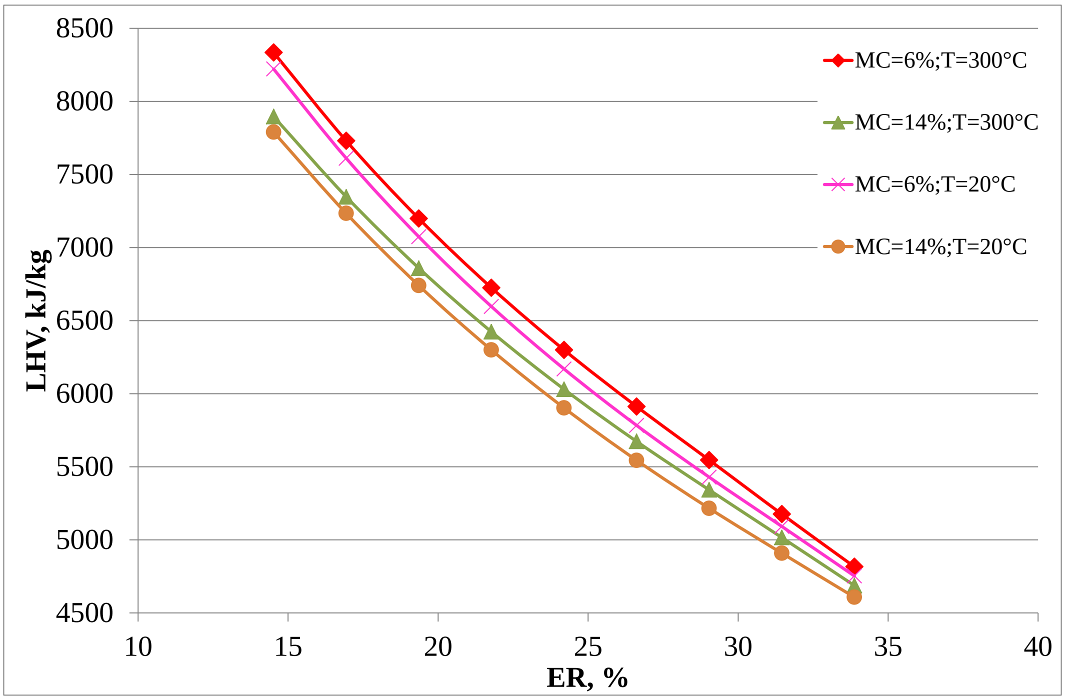

Figure 11 Lower heating value of the syngas for two values of the biomass moisture content and gasifying air temperature.

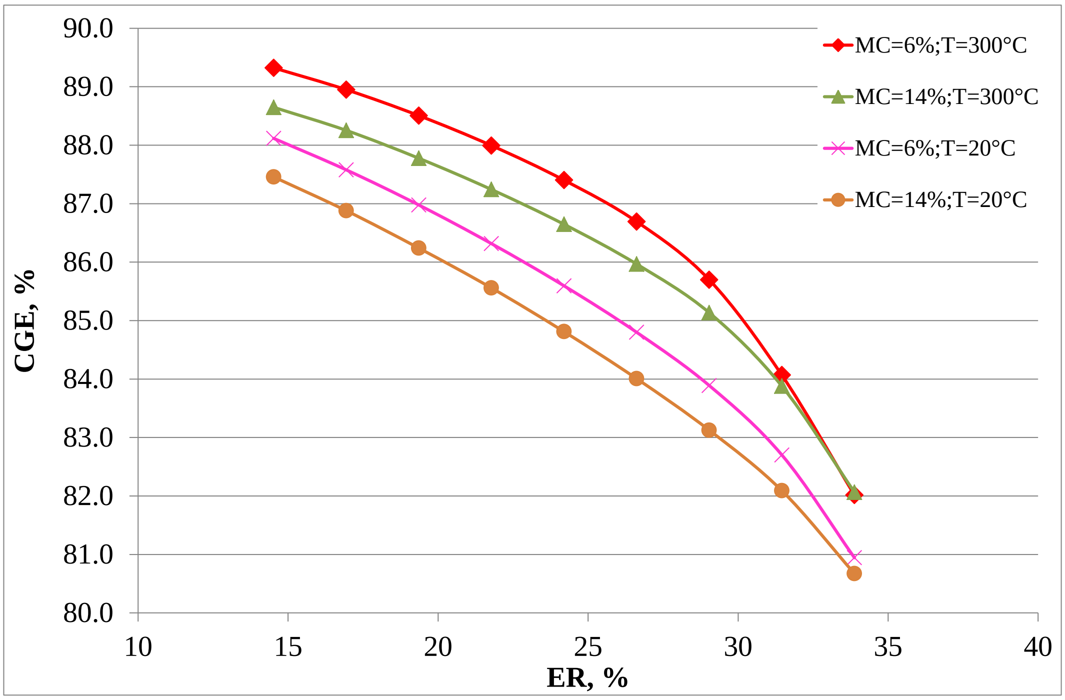

Figure 12 Cold gasification efficiency for two values of the biomass moisture content and gasifying air temperature.

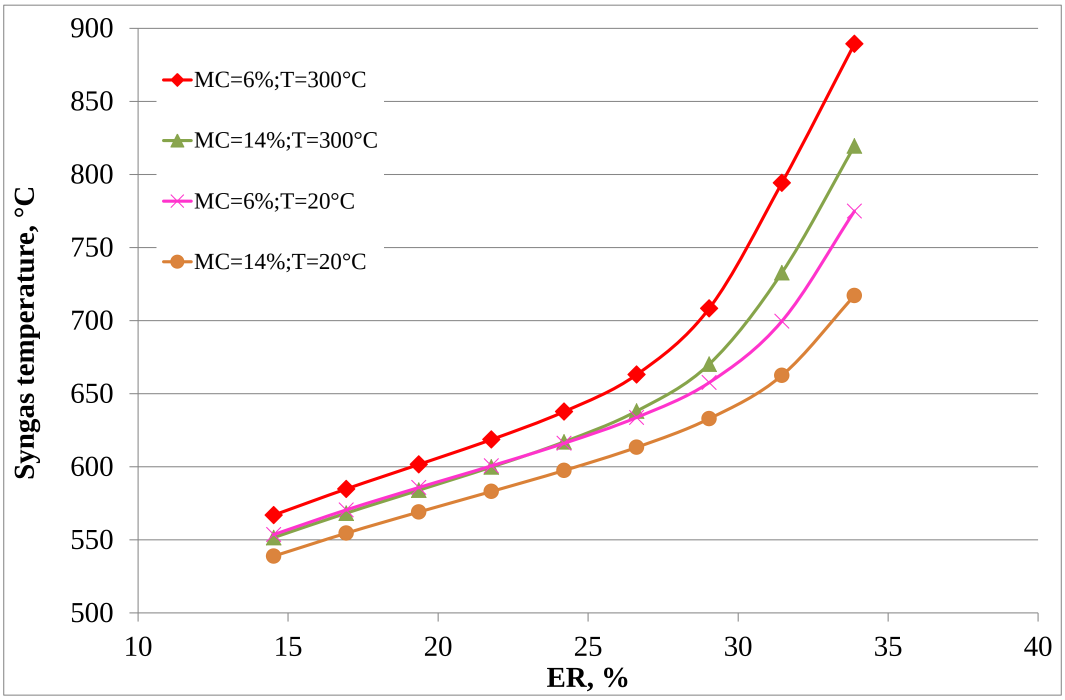

Figure 13 Syngas temperature at the outlet of the gasifier for two values of the biomass moisture content and gasifying air temperature.

5.3 Comparison of the simulated results with literature data

It is interesting to compare the simulated results presented in the previous section with the data that are available in the wide scientific literature. ~~In order to avoid the use of heterogeneous results achieved with markedly different hypotheses, we have taken into account only results that are obtained with equilibrium mathematical modelling and concern explicitly small-scale biomass downdraft gasifiers [23].~~ In order to make a reasonable comparison, we have taken into account only results that are obtained with equilibrium mathematical modelling and concern explicitly small-scale biomass downdraft gasifiers [23]. Moreover, further experimental reference [42] has been taken into account for the comparison. As previously mentioned the simulations have been performed considering biomass characteristics, gasifying air temperature and ER (see Table 4).

Table 4 Ultimate and proximate analyses of biomass for the literature comparison [42].

Proximate Analysis (wt%)		**Ultimate Analysis (wt%)**	
Moisture	5.76 %	Carbon	48.64 %
Fixed Carbon	14.4 %	Hydrogen	5.64 %
Volatile Matter	78.76 %	Nitrogen	0.52 %
Ash	1.08 %	Sulphur	0.03 %
		Oxygen	44.09 %
Higher heating value (MJ/kg)	18.94		
Gasifying air temperature (°C)	20		

The results of the comparison, executed considering three values of ER, are summarized in Figure 14, where it is possible to note a good agreement between current simulated results and the references ones. The maximum relative error of H_2, CO and CO_2 molar concentration on dry basis between the current results and those of [23] is about 9 %, 4 % and 7 %, respectively. If the comparison is executed with the experimental reference [42], the maximum relative error is about 7 %, 4 % and 5.5 %, respectively. As previously mentioned in section 5.1, large differences are present concerning methane whose simulated predictions is close to zero. This depends on the fact that the hypothesis of equilibrium for large values of ER (as those used in this comparison) practically implies the complete conversion of methane into hydrogen and carbon monoxide [38-39], even if some incomplete conversion of pyrolysis products can occur in real operative conditions [23].

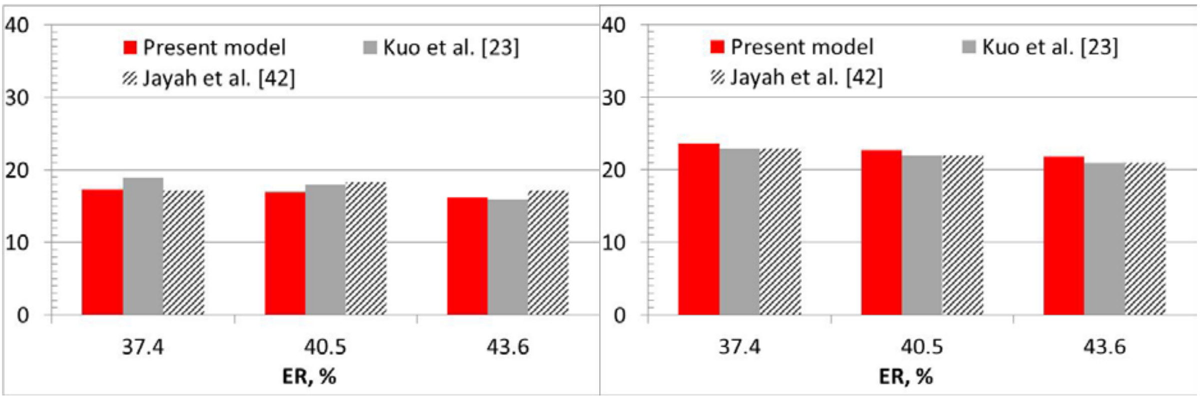

(a) H_2 molar content (b) CO molar content

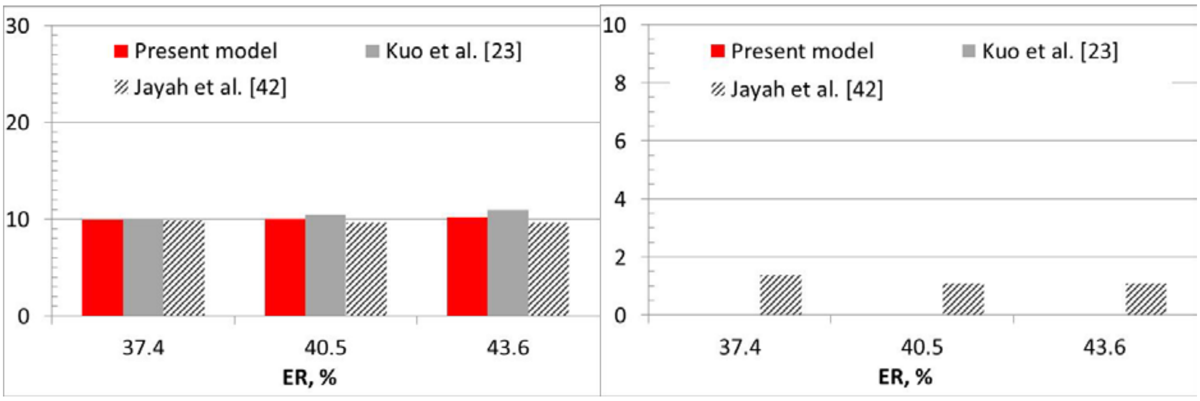

(c) CO_2 molar content (d) CH_4 molar content

Figure 14 Comparison of (a)H_2, (b) CO, (c) CO_2, (d) CH_4 concentration between present and literature data.

6. Conclusions and Future Remarks

In this paper, a detailed numerical model developed with Aspen Plus® for an experimental full-scale biomass gasification plant has been proposed, simulating the gasification process with a kinetic free equilibrium approach.

The model has been implemented with all the measured plant data, such as the exact geometrical and performance characteristics of the plant equipment and the control operative logics. This approach assured to obtain a good matching between the simulation results and the plant data in terms of syngas composition and energy performance of the gasification process. In particular, the syngas composition is well simulated and predicted except for the hydrogen and methane components, because the equilibrium assumption of the model implies the complete conversion of methane into hydrogen. The other parameters, such as the LHV of the syngas and the CGE, are estimated by the simulation model with an average percentage error lower than 7 %.

Once the reliability of the simulation model has been demonstrated with the experimental results, it has been used to analyse the operative behavior and energy performance with respect to some important plant parameters. The most meaningful results are summarized below:

- ~~By~~ by recovering the sensible heat of the syngas at the outlet of the gasifier, it is possible to obtain high values of the gasifying air temperature and an improvement of the overall gasification performances.
- The adoption of dried biomass with higher LHV assures higher gasification efficiencies with larger production of CO.
- The decrease of ER from about 35 % to about 15 % implies an increase of the gasification efficiency by about 6-7 % in function of MC and gasifying air temperature.
- An increase of about 300 °C of the gasifying air temperature assures an improvement of two percentage points of the gasification efficiency.
- As a whole, the influence of MC on the gasifier performance is lower than that of the gasifying air temperature.

The simulation model here presented allows to develop other investigations about some modified layouts of the experimental gasification plant:

- the syngas suction fan can be moved upstream the gasifier in order to obtain a pressurized gasification process;

- the insertion within the simulation model of a specific external routine for the performance assessment of the internal combustion engine;
- the flowing of some syngas through the gasifier to combine air gasification with CO_2 gasification.

APPENDIX A

A.1 Calculation of the pressure drop of the syngas across the gasifier

The pressure drop of the air/syngas across the gasifier (ΔP [Pa]) has been estimated with the Ergun equation for flow through a randomly packed bed of spheres as follows [43]:

$$\Delta P = \left(150 \frac{(1-\varepsilon)^2}{\varepsilon^3} \frac{\mu_i}{d_p^2} u_i + 1.75 \frac{(1-\varepsilon)}{\varepsilon^3} \frac{\rho_i}{d_p} u_i^2 \right) l \quad \text{(A.1)}$$

A.2 Calculation of the heat loss of the gasifier to the environment

The reactor is constituted by a stainless steel shell, which is internally protected by a refractory layer. The external surface of the reactor is insulated by ceramic fiber insulation that is protected by an aluminum cover. The procedure for the estimation of the thermal losses from the gasifier into the environment is described below [44-46]:

$$\dot{Q} = \frac{T_r - T_e}{R_{tot}} \quad \text{(A.2)}$$

R_{tot} can be calculated as follows:

$$R_{tot} = R_i + R_{c1} + R_{c2} + R_{c3} + \left(\frac{1}{R_e} + \frac{1}{R_r} \right) \tag{A.3}$$

where the thermal resistances are summarized in Table A1.

Table A1 Thermal resistances of the gasifier.

$R_i = \frac{1}{\alpha_i \pi D_i L}$
$R_{c1} = \frac{ln\left(\frac{D_{e\_refractory}}{D_i}\right)}{2\pi k_{refractory} L}$
$R_{c2} = \frac{ln\left(\frac{D_{e\_shell}}{D_{e\_refractory}}\right)}{2\pi k_{shell} L}$
$R_{c3} = \frac{ln\left(\frac{D_{e\_insulation}}{D_{e\_shell}}\right)}{2\pi k_{insulation} L}$
$R_e = \frac{1}{\alpha_e \pi D_{e\_insulation} L}$
$R_r = \frac{1}{\alpha_r \pi D_{e\_insulation} L}$

The evaluation of α_i [W/m^2 K] for the convective heat exchange between the air/syngas and the internal surface of the refractory layer is executed with the following expression:

$$\alpha_i = \frac{Nu_i k_i}{D_i} \tag{A.4}$$

where

$$Nu_i = 0.023 Re_i^{0.8} Pr_i^{1/3} \tag{A.5}$$

$$Re_i = \frac{\rho_i \, u_i \, D_i}{\mu_i} \tag{A.6}$$

$$Pr_i = \frac{Cp_i \, \mu_i}{k_i} \tag{A.7}$$

α_e [W/m^2 K] is calculated considering the wind flow across the cylindrical shell using the relation of Churchill-Bernstein:

$$\alpha_e = \frac{Nu_a \, k_a}{D_{e\_insulation}} \tag{A.8}$$

where

$$Nu_a = 0.3 + 0.62 \frac{Re_a^{0.5} Pr_a^{1/3}}{\left[1 + \left(0.4 / Pr_a^{2/3}\right)\right]^{0.25}} \left[1 + \left(\frac{Re_a}{282000}\right)^{5/8}\right]^{0.8} \tag{A.9}$$

$$Re_a = \frac{\rho_a u_a D_{e\_insulation}}{\mu_a} \tag{A.10}$$

$$Pr_a = \frac{Cp_a \, \mu_a}{k_a} \tag{A.11}$$

The evaluation of the radiative heat exchange between the cover of the external thermal insulation of the gasifier and the environment has been executed considering an equivalent coefficient of convective heat exchange. Hence, the evaluation of α_r is obtained with the following expression:

$$\alpha_r = E_m \sigma \left(T_p + T_e\right)\left(T_p^2 + T_e^2\right) \tag{A.12}$$

APPENDIX B

The experimental data that have been used for the simulation with the Aspen Plus® model are summarized in Table B1.

Table B1 Experimental data used in the Aspen Plus® simulation

ER, %	Gasifying air temperature at the inlet of the reactor, °C	Biomass moisture content, %
34.9	252	5.6
33.2	280	5.6
33.7	328	6.5
28.9	375	6.5
34.0	414	6.5
28.9	284	8.3
32.0	351	8.3
31.3	401	7.4
33.6	422	7.4
20.4	427	4.8
36.9	350	9.8
35.2	491	7.9
38.1	292	7.9
36.8	384	10.1
38.1	206	4.7
37.9	362	7.1
35.4	362	7.6
35.5	400	7.6
37.3	425	5.5
30.4	321	8.7
37.4	394	8.7
37.9	434	6.2
37.2	450	6.2

ACKNOWLEDGMENTS

The authors wish to thank Regione Toscana for financial support of the project ICGBL through the fund POR CReO FESR 2007-2013 (Attività 1.5.a - 1.6). Moreover, the authors thank ENEL SpA – Engineering & Research for the use of Aspen Plus®.

REFERENCES

[1] Grassi G, Gosse G, Dos-Santos G. Biomass for energy and industry. London: Elsevier Applied Science; 1990.

[2] Wang L, Weller CL, Jones DD, Hanna MA. Review - Contemporary issues in thermal gasification of biomass and its application to electricity and fuel production. Biomass and Bioenergy 2008; 32: 573-581.

[3] Kirubakaran V, Sivaramakrishnan V, Nalini R, Sekar T, Premalatha M, Subramanian P. A review on gasification of biomass. Renewable and Sustainable Energy Reviews 2009: 13: 179-186.

[4] Asadullah M. Barriers of commercial power generation using biomass gasification gas: a review. Renewable and Sustainable Energy Reviews 2014; 29: 201-215.

[5] Ahmad AA, Zawawi NA, Kasim FH, Inayat A. Assessing the gasification performance of biomass: a review on biomass gasification process conditions, optimization and economic evaluation. Renewable and Sustainable Energy Reviews 2016; 53: 1333-1347.

[6] Janajreh I, Al Shrah M. Numerical and experimental investigation of downdraft gasification of wood chips. Energy Conversion and Management 2013; 65: 783-792.

[7] Puig-Arnavat M, Bruno JC, Coronas A. Review and analysis of biomass gasification models. Renewable and Sustainable Energy Reviews 2010; 14: 2841-2851.

[8] Baruah D, Baruah DC. Modelling of biomass gasification: a review. Renewable and Sustainable Energy Reviews 2014; 39: 806-815.

[9] Patra TK, Sheth PN. Biomass gasification models for downdraft gasifier: a state-of-the-art review. Renewable and Sustainable Energy Reviews 2015; 50: 583-593.

[10] Sharma AKr. Modeling and simulation of a downdraft biomass gasifier 1. Model development and validation. Energy Conversion and Management 2011; 52: 1386-1396.

[11] Sharma S, Sheth PN. Air–steam biomass gasification: Experiments, modeling and simulation. Energy Conversion and Management 2016; 110: 307–318.

[12] Ghassemi H, Shahsavan-Markadeh R. Effects of various operational parameters on biomass gasification process; a modified equilibrium model. Energy Conversion and Management 2014; 79: 18–24.

[13] Andrés Z, Mendiburu AZ, Carvalho Jr JA, Zanzi R, Coronado CR, Silveira JL. Thermochemical equilibrium modeling of a biomass downdraft gasifier: Constrained and unconstrained non-stoichiometric models. Energy 2014; 71: 624–637.

[14] Ramzan N, Ashraf A, Naveed S, Malik A. Simulation of hybrid biomass gasification using Aspen plus: A comparative performance analysis for food, municipal solid and poultry waste. Biomass and Bioenergy 2011; 35: 3962-3969.

[15] Fu Z, Zhang Y, Liu H, Zhang B, Li B. Simulation analysis of biomass gasification in an autothermal gasifier using Aspen Plus. Cleaner Combustion and Sustainable World 2012; 479-483, Springer Berlin Heidelberg.

[16] Doherty W, Reynolds A, Kennedy D. The effect of air preheating in a biomass CFB gasifier using ASPEN Plus simulation. Biomass and Bioenergy 2009; 33: 1158-1167.

[17] Doherty W, Reynolds A, Kennedy D. Simulation of a circulating fluidised bed biomass gasifier using Aspen Plus - A performance analysis. Proc. 21st International Conference on

Efficiency, Cost, Optimization, Simulation and Environmental Impact of Energy Systems, Krakow, Poland, 2008, 1241-1248.

[18] Doherty W, Reynolds A, Kennedy D. Aspen Plus Simulation of Biomass Gasification in a Steam Blown Dual Fluidised Bed, Book Chapter: Materials and processes for energy: communicating current research and technological developments, A. Méndez-Vilas (Ed.), Formatex Research Centre, 2013.

[19] Abdelouahed L, Authier O, Mauviel G, Corriou JP, Verdier G, Dufour A. Detailed modeling of biomass gasification in dual fluidised bed reactors under Aspen Plus. Energy Fuels 2012; 26: 3840-3855.

[20] Francois J, Abdelouahed L, Mauviel G, Feid M, Rogaume C, Mirgaux O, Patisson F, Dufour A. Estimation of the energy efficiency of a wood gasification CHP plant using Aspen Plus. Chemical Engineering Transactions 2012; 29: 769-774.

[21] Francois J, Abdelouahed L, Mauviel G, Patisson F, Mirgaux O, Rogaume C, Rogaume Y, Feid M, Dufour A. Detailed process modeling of a wood gasification combined herat and power plant. Biomass and Bioenergy 2013; 51: 68-82.

[22] Nikoo MB, Mahinpey N. Simulation of biomass gasification in fludized bed reactor using Aspen Plus. Biomass and Bioenergy 2004; 32: 1245-1254.

[23] Kuo PC, Wu W, Chen WH. Gasification performances of raw and torrified biomass in a dowdraft fixed bed gasifier using thermodynamic analysis. Fuel 2014; 117: 1231-1241.

[24] Mathieu P, Dubuisson R. Performance analysis of a biomass gasifier. Energy Conversion and Management 2002; 43: 1291-1299.

[25] Damartzis Th, Michailos S, Zabaniotou A. Energetic assessment of a combined heat and power integrated biomass gasification-internal combustion engine system by using Aspen Plus. Fuel Processing Technology 2012; 95: 37-44.

[26] Sreejith CC, Muraleedharan C, Arun P. Performance prediction of steam gasification of wood using an Aspen Plus thermodynamic equilibrium model. International Journal of Sustainable Energy 2014; 33: 416-434.

[27] Tremel A, Becherer D, Fendt D, Gaderer M, Spliethoff H. Performance of entrained flow and fluidised bed biomass gasifiers on different scales. Energy Conversion and Management 2013; 69: 95–106.

[28] Do TX, Lim Yi, Yeo H, Lee Ud, Choi Yt, Song Jh. Techno-economic analysis of power plant via circulating fluidised-bed gasification from woodchips. Energy 2014; 70: 547-560.

[29] Beheshti SM, Ghassemi H, Shahsavan-Markadeh R. Process simulation of biomass gasification in a bubbling fluidised bed reactor. Energy Conversion and Management 2015; 94: 345-352.

[30] Tapasvi D, Kempegowda RS, Tran KQ, Skreiberg O, Gronli M. A simulation study on the torrefied biomass gasification. Energy Conversion and Management 2015; 90: 446–457.

[31] Parvez AM, Mujtaba IM, Wu T. Energy, exergy and environmental analyses of conventional, steam and CO_2-enhanced rice straw gasification. Energy 2016; 94: 579-588.

[32] Adeyemi I, Janajreh I. Modeling of the entrained flow gasification: Kinetics-based ASPEN Plus model. Renewable Energy 2015; 82: 77-84.

[33] Font Palma C. Modelling of tar formation and evolution for biomass gasification: A review. Applied Energy 2013; 111: 129-141.

[34] Li C, Suzuki K. Tar property, analysis, reforming mechanism and model for biomass gasification - An overview. Renewable and Sustainable Energy Reviews 2009; 13: 594-604.

[35] Technical Report "Sampling and analysis of tar and particles in biomass producer gases" Prepared under CEN BT/TF 143 "Organic contamination ("tar") in biomass producer gases".

[36] UNI CEN/TS 15439:2008 “Biomass gasification, Tar and particles in product gases, Sampling and analysis”, European code.

[37] ISO 5167-2:2003 “Measurement of fluid flow by means of pressure differential devices inserted in circular cross-section conduits running full -- Part 2: Orifice plates”, International code.

[38] Jarungthammachote S, Dutta A. Thermodynamic equilibrium model and second law analysis of a downdraft waste gasifier. Energy 2007; 32: 1660-1669.

[39] Baratieri M, Baggio P, Fiori L, Grigiante M. Biomass as an energy source: Thermodynamic constraints on the performance of the conversion process. Bioresource Technology 2008; 99: 7063-7073.

[40] Zainal ZA, Rifau A, Quadir GA, Seetharamu KN. Experimental investigation of a downdraft biomass gasifier. Biomass and Bioenergy 2002; 23: 283-289.

[41] Melgar A, Pe´rez JF, Laget H, Horillo A. Thermochemical equilibrium modelling of a gasifying process. Energy Conversion and Management 2007; 48: 59-67.

[42] Jayah TH, Aye L, Fuller RJ, Stewart DF. Computer simulation of a downdraft wood gasifier for tea drying. Biomass and Bioenergy 2003; 25: 459–469.

[43] Rhodes M. Introduction of Particle Technology. Chichester: John Wiley & Sons; 2008.

[44] Bejan A, Tsatsaronis G, Moran M. Thermal Design and Optimization. Chichester: John Wiley & Sons; 1995.

[45] Bejan A. Convection Heat Transfer. Chichester: John Wiley & Sons; 2013.

[46] Mills AF. Heat Transfer. Homewood: Irwin Inc.; 1992.